



Article

Plasma membrane-associated calcium signaling modulates zinc homeostasis in *Arabidopsis*

Yanjun Fang^{a,b,1}, Chuanfeng Ju^{a,1}, Laiba Javed^{a,1}, Chenyu Cao^a, Yuan Deng^a, Yaqi Gao^a, Xuanyi Chen^a, Lv Sun^a, Yusheng Zhao^b, Cun Wang^{a,c,*}

^aState Key Laboratory for Crop Stress Resistance and High-Efficiency Production, College of Life Sciences, Northwest Agriculture & Forestry University, Yangling 712100, China

^bState Key Laboratory of Plant Cell and Chromosome Engineering, Institute of Genetics and Developmental Biology, Chinese Academy of Sciences, Beijing 100101, China

^cInstitute of Future Agriculture, Northwest Agriculture & Forestry University, Yangling 712100, China

ARTICLE INFO

Article history:

Received 5 September 2024

Received in revised form 7 January 2025

Accepted 7 February 2025

Available online 13 February 2025

Keywords:

Zinc

Ca²⁺-CBL-CIPK

ZIP12

Arabidopsis

ABSTRACT

Zinc (Zn) is a crucial micronutrient for all organisms, and its deficiency can significantly hamper crop yield and quality. However, the understanding of the regulatory mechanisms involved in plant Zn signal perception and transduction remains limited. In this study, we discovered that the Ca²⁺-CBL1/4/5/8/9-CIPK3/9/23/26-ZIP12 signaling module effectively responds to Zn deficiency and regulates Zn homeostasis in *Arabidopsis thaliana*. Furthermore, we determined that CIPK3/9/23/26 interact with the Zn transporter ZIP12 and phosphorylate it primarily at Ser185. This phosphorylation event was crucial for the stability of the ZIP12 protein, suggesting that it regulates the function of ZIP12 in Zn transport. Collectively, our findings identify a plasma membrane-associated calcium signaling pathway that regulates Zn homeostasis in *Arabidopsis thaliana*. This pathway represents a promising target for molecular breeding approaches aimed at developing crops with enhanced tolerance to Zn deficiency.

© 2025 The Authors. Published by Elsevier B.V. and Science China Press. This is an open access article under the CC BY license (<http://creativecommons.org/licenses/by/4.0/>).

1. Introduction

Zn is a crucial trace element essential for plant growth and development, as well as for animals and humans. Zn plays a vital role in gene expression regulation, protein synthesis, photosynthesis, respiration, hormone regulation, signal transduction, and stress responses [1–3]. Recent studies found that Zn plays a crucial ‘second messenger’ role in legume root nodules, linking environmental changes to transcription factor control of nodule metabolic activity [4]. According to statistics, approximately 50% of the world’s arable land is deficient in Zn [5]. When plants lack Zn, they display significant symptoms such as shortened plants, chlorotic leaves, deformed small leaves, and abnormal fruit development. This deficiency is one of the significant limiting factors for crop yield and quality [6,7].

The transcription factors bZIP19/23 are recognized as Zn sensors [8,9]. In Zn-deficiency conditions, bZIP19 and bZIP23 activate the expression of target genes by binding to the Zn deficiency response element in the promoter. The target genes of bZIP19/23 encompass a select group of Zn homeostasis genes that play crucial

roles in regulating Zn absorption, transportation, and distribution processes. Notably, these targets include members belonging to the ZIP transporter family and the nicotianamine synthase (NAS) family, both of which are integral to Zn metabolism [10]. There are 15 members of the ZIP/IRT family in *Arabidopsis*, namely AtZIP1–AtZIP12 and AtIRT1–3 [11]. At least 10 ZIPs (ZIP1–4, 6, 7, 9, 11–12 and IRT3) can compensate for the Zn-deficiency growth phenotype of *Saccharomyces cerevisiae* *zrt1zrt2* mutant [8,12–15]. Zn deficiency induces the transcriptional expression of ZIP1/3/4/5/6/9/10/12 and IRT3, but only ZIP3/4/9/12 and IRT3 are mainly involved in Zn absorption in plants under Zn deficiency conditions [8,12,14,15]. Notably, ZIP12 displays a remarkable upregulation, by several hundred-fold, in *Arabidopsis* under Zn-deficiency conditions. This heightened expression of ZIP12 is similarly observed in various crops, including rice, maize, and barley, when subjected to Zn deficiency [8,9,11,14,16].

Calcium (Ca²⁺) is a crucial regulatory factor for plant growth, development, and stress responses [17]. When plants encounter environmental changes, the concentration of Ca²⁺ in the cytoplasm rapidly alters, and the Ca²⁺ signals triggered by various stimuli differ in terms of duration, space, frequency, and amplitude [18,19]. The CBL-CIPK signaling system, serving as a unique Ca²⁺ sensor in plants, plays a pivotal role in plants’ responses to drought, salinity, nutrition, and other stresses [20]. Recently, reports have

* Corresponding author.

E-mail address: cunwang@nwfafu.edu.cn (C. Wang).

¹ These authors contributed equally.

emphasized the crucial role played by both Ca²⁺-dependent (CBL-CIPK) and Ca²⁺-independent (FLS2-BAK1-BIK1/PBL1) mechanisms in regulating cytoplasmic Ca²⁺ homeostasis, thereby maintaining a delicate balance between plant growth and immunity [21]. However, the extent to which Ca²⁺-CBL-CIPK regulates Zn uptake, transport and distribution in plants remains to be explored.

In this study, we discovered that the plasma membrane-localized Ca²⁺-CBL1/4/5/8/9-CIPK3/9/23/26 signaling regulates Zn homeostasis. The *cbl1/4/5/8/9* and *cipk3/9/23/26* mutants displayed significant tolerance to Zn deficiency. Furthermore, CIPK3/9/23/26 interacted with the plasma membrane-localized Zn transporter ZIP12, phosphorylating the Ser185 site of ZIP12, which is crucial for determining the stability of ZIP12 protein. In summary, our findings identified the mechanism of the Ca²⁺-CBL1/4/5/8/9-CIPK3/9/23/26-ZIP12 signaling module regulating Zn homeostasis under Zn deficiency, and revealed the adaptive response mechanism of plants to Zn deficiency.

2. Materials and methods

2.1. Plant materials and growth conditions

Arabidopsis thaliana wild-type (WT; ecotype Columbia-0), the T-DNA insertion lines *cbl7* (SAIL-100-F05), *cbl10* (SALK_056042), *cipk3* (SALK_137779), *cipk9* (SALK_014699), *cipk23* (SALK_036154), *cipk26* (SALK_000085). The higher-order mutants of *cbl1/4/5/8/9* were previously described [22]. And *zip4* (SALK_145371), *zip9-1* (SALK_090345), *zip9-2* (SALK_074682), *zip12-1* (SALK_137184), and *zip12-2* (SALK_118705) were obtained from Nottingham *Arabidopsis* Stock Centre (NASC); The mutants used are listed in Tables S1 and S2 (online).

Arabidopsis seeds were surface-sterilized and then stratified for 3 d at 4 °C. The seeds were grown on a nutrient medium consisting of 1.2% agar (Sigma-Aldrich, A1296), 2% sucrose, and full-strength Hoagland nutrient solution (5 mmol/L KNO₃, 5 mmol/L Ca(NO₃)₂, 2 mmol/L MgSO₄, 1 mmol/L NH₄H₂PO₄, 20 μmol/L MnSO₄, 3 μmol/L H₃BO₃, 1 μmol/L (NH₄)₆Mo₇O₂₄, 0.4 μmol/L ZnSO₄, 0.2 μmol/L CuSO₄, 20 μmol/L Fe (III)-EDTA) at pH 5.75–5.85. To conduct the Zn deficiency germination experiment, ZnSO₄ was not added to the Zn-deficiency (low Zn) medium, but 50 μmol/L EDTA-Na₂ was added to eliminate the influence of Zn in the agar. As a control, 50 μmol/L EDTA-Na₂ was also added to the Hoagland medium. The plants were grown on vertical plates at 21 °C for 10 d under a 16 h light/8 h dark cycle. The experiment was repeated in 3 dishes each time, 6 plants per genotype each time, and repeated independently for 3 times, a total of 18 plants.

For hydroponic conditions, *Arabidopsis* seedlings grown on Hoagland medium for 7 d were transferred to 1/5 Hoagland nutrient solution for 2 weeks, then they were transferred to 1/5 Hoagland nutrient solution without ZnSO₄ for Zn deficiency and 1/5 Hoagland nutrient solution as control for 2 weeks under short-day conditions (8 h:16 h, light: darkness) at 22 °C. Each pot can cultivate 4 kinds of plants, a total of 12 plants, each of 3 plants, a total of 3 repeated experiments. And the solution is changed every three days.

For the Zn deficiency compensation phenotype test, surface-sterilized seeds were germinated on Zn-deficiency medium for 5 d and then transplanted onto Hoagland medium for another 5 d under a 16-hour light/8-hour dark cycle. To conduct high-Zn treatments, surface-sterilized seeds were sown on half-strength MS medium containing 1% (w/v) sucrose and 1% (w/v) agar (pH adjusted to 5.7 using Tris). After 4 d of growth, seedlings were transferred to 1/2 MS medium with 400 μmol/L ZnSO₄ or 500 μmol/L ZnSO₄ for 6 d under a 16-hour light/8-hour dark cycle. The experiments were repeated in 3 dishes each time, 6 plants per

genotype each time, and repeated independently for 3 times, a total of 18 plants. For soil culture, 7-day-old seedlings growing on Hoagland medium were transplanted to nutrient-rich soil (Pindstrup substrate, Denmark) and then grown under normal light conditions (100 μmol m⁻² s⁻¹) and a long-day cycle (16 h:8 h, light: darkness) at 22 °C.

2.2. Plasmid construction

To construct the overexpression vector, the full-length coding sequences (CDS) of ZIP12 were cloned into the pCAMBIA-1300-GFP vector with the 35S promoter. Mutagenesis of ZIP12^{S185A} and ZIP12^{S185D} were performed using the Tiangen Rapid Site-Directed Mutagenesis Kit (Tiangen, Beijing, China). The full-length CDS of ZIP12 was cloned into the GUS-cYFP vector and the pCAMBIA-1300 GUS-cLUC vector with the 35S promoter, respectively, for the BiFC and LCI analyses [23]. CIPK3/9/23/26-nYFP and CIPK3/9/23/26-nLUC were described previously [24,25]. To construct the recombinant protein vectors, ZIP12-Loop (427–600 bp) was amplified and cloned into the pGEX4T-1 vectors to obtain GST-ZIP12-Loop [26]. CIPK3/9-N/23/26-GST was described previously [24,25]. The primers used are listed in Table S3 (online).

2.3. Elemental analysis

The samples were taken from the shoots and roots of the plants and washed three times with double distilled water to remove ions adsorbed on the surface of the plants. Then dried overnight at 65 °C and weighed, and then heated to 120 °C in pure nitric acid solution. Hydrogen peroxide was added to make the digestion sufficient, and the temperature was raised to 160 °C for one hour. Finally, the samples were then dissolved in double distilled water and analyzed by inductively coupled plasma mass spectrometry (ICP-MS).

2.4. Semi-quantitative RT-PCR and quantitative real-time RT-PCR

To extract total RNA from 10-day-old seedlings, we used an RNA simple total RNA kit (Tiangen). First-strand cDNA was synthesized from the total RNA using the HiScript II Q RT SuperMix for qPCR (+gDNA wiper) (Vazyme, Shanghai, China) and the HiScript II 1st Strand cDNA Synthesis Kit (+gDNA wiper) for semi-quantitative RT-PCR (Vazyme). RT-qPCR was performed according to the instructions provided with the real-time PCR instrument (CFX connect, Bio-Rad, USA) using the ChamQ SYBR qPCR Master Mix (Vazyme). Each sample was quantified in at least three portions and normalized with the *ACTIN2* gene as an internal control. The specific primers used are listed in Table S3 (online).

2.5. BiFC assay

The BiFC assay was conducted based on a published method [23]. In summary, a buffer was used to adjust the concentration of *Agrobacterium tumefaciens* to a specific absorbance at 600 nm. The combinations of CIPK3/9/23/26-nYFP with ZIP12-cYFP, CIPK3/9/23/26-nYFP with GUS-cYFP, and ZIP12-cYFP with GUS-nYFP were injected into the leaves of *N. benthamiana*. After 48 h of expression, the fluorescence signals were observed under a confocal laser scanning microscope (Olympus IX83-FV3000).

2.6. LCI assay

The LCI assay was based on a published method [23]. Briefly, combinations of CIPK3/9/23/26-nLUC with ZIP12-cLUC, CIPK3/9/23/26-nLUC with GUS-cLUC, and ZIP12-cLUC with GUS-nLUC were co-injected into *N. benthamiana* leaves. After

48 h of expression, the LCI signals were detected using a cooled charge-coupled device (Princeton, Lumazone Pylon 2048B).

2.7. Co-immunoprecipitation assay

The Co-immunoprecipitation (Co-IP) assay was performed according to a previously published protocol [25]. To extract the total proteins, 10-day-old *pro35S::GUS-FLAG/pro35S::ZIP12-GFP* and *pro35S::proCIPK26-FLAG/GFP* transgenic *Arabidopsis* roots were ground in IP buffer (50 mmol/L Tris-HCl, pH 7.6, 150 mmol/L NaCl, 10% glycerol, 5 mmol/L MgCl₂, 0.5% NP-40, 1 mmol/L phenylmethylsulfonyl fluoride, 1 × protease inhibitor cocktail, and 1 mmol/L DTT). The ground samples were mixed with anti-GFP agarose beads (Proteintech), washed three times with PBS buffer, and eluted with SDS-PAGE loading buffer. The eluate was then subjected to SDS-PAGE for an immunoblot assay. CIPK26 and ZIP12 were detected with anti-FLAG antibodies and anti-GFP antibodies (TransGen Biotech).

2.8. Protein kinase assays

The *in vitro* protein kinase assay was performed as described previously [27]. ZIP12-Loop and site-mutated proteins were incubated with CIPK3/9/23/26-GST in kinase reaction buffer containing 2.5 mmol/L MgCl₂, 20 mmol/L Tris-HCl (pH 7.2), 2.5 mmol/L MnCl₂, 1 mmol/L DTT, 0.5 mmol/L CaCl₂, 50 mmol/L ATP, and 1 μCi (γ -³²P) ATP at 30 °C for 30 min. The reaction was then heated at 100 °C for 5 min in 5 × loading buffer. The proteins were separated by SDS-PAGE and the signals were detected using a Typhoon 9410 imager (Cytiva Sweden AB, Uppsala, Sweden).

For the *in vivo* protein kinase assay, *pro35S::ZIP12-GFP* and *pro35S::ZIP12^{S185A}-GFP* constructs were transformed into WT or *cipk3/9/23/26* plants using *Agrobacterium tumefaciens*. The T3 seedlings were subjected to Zn-deficiency conditions for 0 h, 6 h, 12 h, 1 d, 3 d and 5 d. Total proteins were extracted using a protein extraction buffer (50 mmol/L Tris-HCl, pH 7.6, 150 mmol/L NaCl, 10% glycerol, 5 mmol/L MgCl₂, 0.5% NP-40, 1 mmol/L phenylmethylsulfonyl fluoride, 1 × protease inhibitor cocktail, and 1 mmol/L DTT) and subsequently enriched using anti-GFP agarose beads (Proteintech) for 2 h at 4 °C. Following enrichment, the beads were washed three times with PBS buffer and mixed with an appropriate volume of 5 × loading buffer. The mixture was then heated at 100 °C for 5 min, and protein expression was assessed via immunoblotting. The phosphorylation signal of ZIP12 was analyzed by Western blot using a phosphoserine-specific antibody (YM3440; ImmunoWay, Plano, TX, USA). Protein quantification was performed using immunoblotting with anti-GFP antibodies (TransGen Biotech, catalog #HT201/#HT801).

2.9. Phylogenetic analysis

All protein sequences were downloaded from NCBI and aligned by MUSCLE algorithm using MEGA X with the specific parameter 'Cluster Method (Iterations1, 2): Neighbor Joining, Cluster Method (Other Iterations): Neighbor Joining' [28]. The phylogenetic trees were constructed by Neighbor Joining method with default settings by MEGA X. The motif logo was generated by WebLogo3 (<https://weblogo.berkeley.edu/logo.cgi>).

2.10. Protein stability analysis

Using T3 stable lines of *pro35S::ZIP12-GFP/zip12* and *pro35S::ZIP12^{S185A}-GFP/zip12*. These transgenic plants were grown on Hoagland medium for 7 d, and then transferred to Zn-deficiency medium for 0 h, 6 h, 12 h, 1 d, 3 d, 5 d, 7 d, 10 d and transferred to Zn-deficiency medium containing 10 μmol/L MG132 or 10 μmol/

L CHX for 0 h, 6 h, 12 h, 1 d, 3 d, 5 d. The proteins were extracted and enriched with anti-GFP agarose beads (Proteintech).

2.11. Subcellular localization of ZIP12

Using T3 stable lines of *pro35S::ZIP12-GFP/zip12*, *pro35S::ZIP12^{S185A}-GFP/zip12* and *pro35S::ZIP12^{S185D}-GFP/zip12* transgenic plants, GFP fluorescence was observed under confocal microscopy (Olympus) after vertical growth for 5 d in Hoagland and Zn-deficiency medium. The excitation wavelength was 488 and 500–540 nm for GFP and 561 and 650–710 nm for PI.

2.12. Yeast functional analysis

Yeast vectors expressing ZIP12 and its variants were transformed into the *Δzrt1/zrt2* yeast strains, respectively. SD-Ura liquid medium (pH = 5.8) containing 6.7 g l⁻¹ YNB (yeast nitrogen base without amino acid), 2% (w/v) D-(+)-galactose and 1% (w/v) agar. For complementation of *Δzrt1/zrt2* the medium was supplemented with or without 5 mmol/L EGTA, and SD-Ura liquid medium was used to culture yeast to OD₆₀₀ = 0.1. Four 10-fold dilution series were established under sterile conditions, and 2.5 μL of each gradient dilution was spotted onto the medium.

2.13. GCAMP6s-based [Ca²⁺]_{cyt} imaging

To visualize Ca²⁺ in the root tip and a portion of the elongation zone (near the root tip) of *GCAMP6s* transgenic seedlings, we followed a specific protocol. The seedlings were grown on Hoagland medium for 4 d and then transferred to Zn-deficiency medium and Hoagland medium (serving as a negative control). The seedlings were then excised with agar and affixed to a slide. GFP signals were collected every 30 s. To record fluorescence images, we excited the sample at 488 nm and collected emissions in the range of 500–540 nm. The scan resolution was set to 1024 × 1024 pixels.

3. Results

3.1. Plasma membrane localized CBL1/4/5/8/9-CIPK3/9/23/26 complex responds to Zn deficiency

The CBL-CIPK complex is a Ca²⁺ sensor involved in various plant life processes [29]. However, whether the CBL-CIPK signaling pathway responds to Zn deficiency remained elusive. Therefore, we used reverse genetics strategy to screen the Zn deficiency phenotype of *cbl* T-DNA insertion mutants, including the Subgroup I members *cbl8*, *cbl1/9*, *cbl1/4/5/9*, *cbl1/4/5/8/9* located on the plasma membrane and the Subgroup II members *cbl2/3*, *cbl6*, *cbl7* and *cbl10* of the CBL family [19]. To conduct this experiment, 50 μmol/L of EDTA-Na₂ was introduced into the Zn-deficiency medium, serving to sequester Zn²⁺ in the agar. Furthermore, to mitigate any potential interference of EDTA-Na₂ with other ions, an equal concentration of 50 μmol/L EDTA-Na₂ was included in the Hoagland medium [9]. We observed that the *cbl1/4/5/9* and *cbl1/4/5/8/9* high-order mutants exhibited significant tolerance compared with the wild type (WT) on Zn-deficiency medium, with longer primary root lengths and a significant increase in fresh weight (Fig. 1a–c). Other *cbls* mutants showed no obvious phenotype compared with WT on Zn-deficiency medium (Fig. S1a–c online). These results indicated that CBL1/4/5/8/9 is involved in the regulation of Zn deficiency and exhibits functional redundancy.

The CBL-type Ca²⁺ sensor proteins regulate signal transduction and function by activating their interacting CIPKs and targeting these kinases to the subcellular locations of their targets [30,31]. It has been reported that CBL1,4,5,8,9 can form a regulatory net-

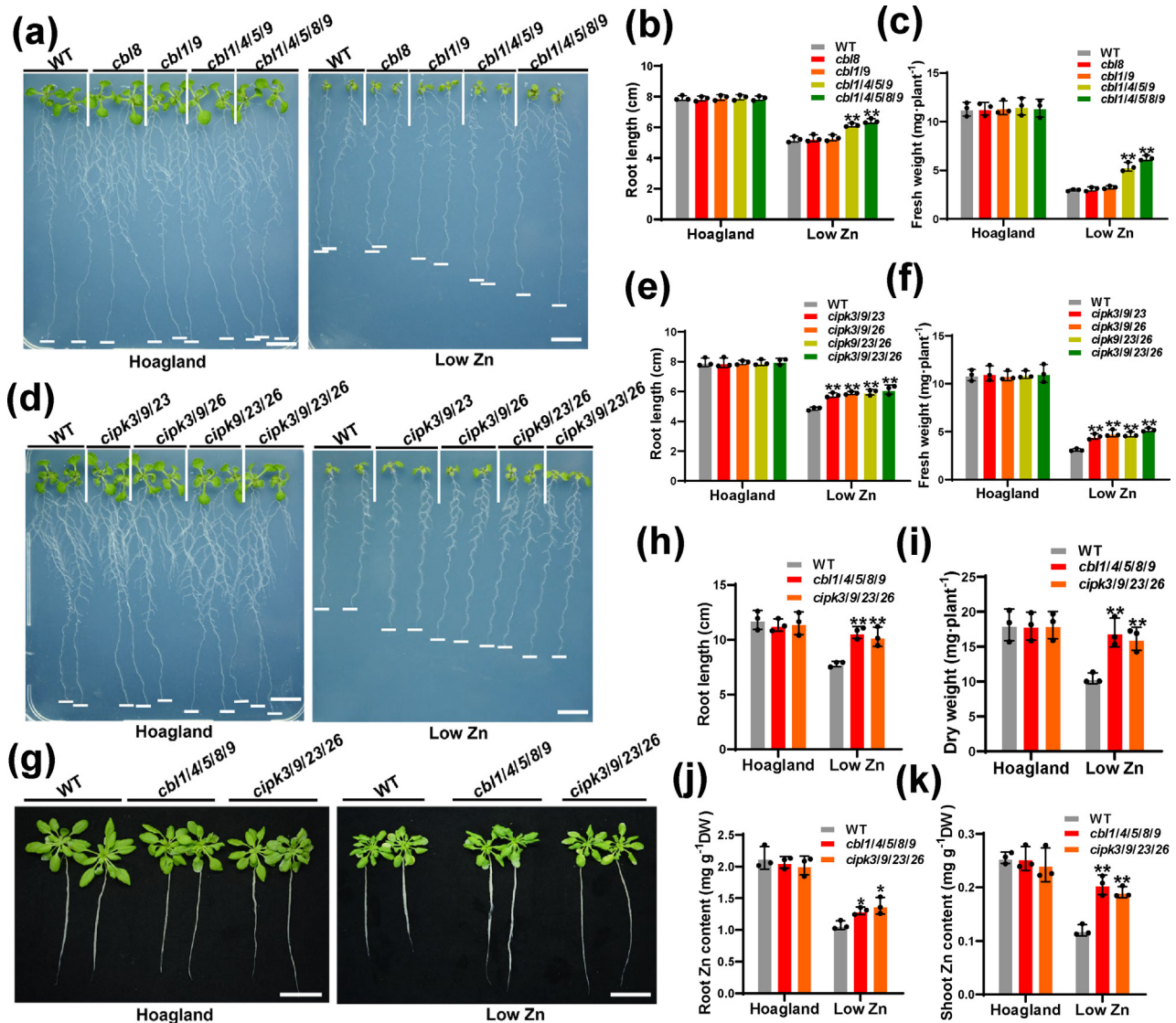


Fig. 1. *cb1/4/5/8/9* and *cipk3/9/23/26* mutants are tolerant to Zn deficiency. (a) Zn-deficiency phenotypes of wild-type (WT) plants and *cb1/8*, *cb1/9*, *cb1/4/5/9*, and *cb1/4/5/8/9* mutants. Plants grew on Hoagland and low Zn medium for 10 d. Scale bars, 1 cm. (b and c) Statistical analysis of the root lengths and fresh weights of the plants shown in (a). (d) Zn-deficiency phenotypes of WT plants and *cipk3/9/23*, *cipk3/9/26*, *cipk9/23/26*, and *cipk3/9/23/26* mutants. Scale bars, 1 cm. (e and f) Statistical analysis of the root lengths and fresh weights of (d). (g) Phenotypic analysis of WT and *cb1/4/5/8/9*, *cipk3/9/23/26* mutant plants in hydroponic culture and treated for 2 weeks with low Zn culture solution. Scale bars, 3 cm. (h and i) Statistical analysis of the root lengths and dry weights of the plants shown in (g). (j and k) Statistical analysis of Zn concentrations of the plants shown in (g). Bars represent the mean \pm SD ($n = 3$ independent biological replicates, 16 seedlings; * $P < 0.05$, ** $P < 0.01$; Student's t test).

work with one or more members of CIPK3,9,23,26 [32]. Therefore, we screened *cipk* T-DNA insertion mutants (*cipk3*, *cipk9*, *cipk23*, *cipk26*, *cipk3/9*, *cipk3/26*, *cipk9/26*, *cipk3/9/23*, *cipk3/9/26*, *cipk9/23/26*, and *cipk3/9/23/26*). Our results showed that the triple mutants *cipk3/9/23*, *cipk3/9/26*, *cipk9/23/26*, and the quadruple mutant *cipk3/9/23/26* were significantly different from WT, with longer primary root lengths and a significant increase in fresh weight (Fig. 1d–f). However, the single mutants *cipk3*, *cipk9*, *cipk23*, *cipk26* and the double mutants *cipk3/9*, *cipk3/26*, *cipk9/26* did not show an obvious Zn deficiency phenotype (Fig. S1d–i online). These results suggested that CIPK3/9/23/26, like CBL1/4/5/8/9, is involved in the regulation of Zn deficiency and has functional redundancy in the Zn deficiency signal transduction pathway.

To further investigate the biological function of CBL-CIPK in response to Zn deficiency, we assayed the concentrations of Zn, Fe, Mn, and Cu in the mutants, both under standard conditions (using 1/5 Hoagland hydroponic solution) and in Zn-deficiency environment (employing 1/5 Hoagland hydroponic solution devoid of

ZnSO₄). Our findings revealed that, under Zn deficiency, the *cb1/4/5/8/9* and *cipk3/9/23/26* mutants displayed remarkable tolerance phenotypes, characterized by elongated root length and increased fresh weight (Fig. 1g–i). Examination of metal concentrations indicated no noteworthy alterations in Fe, Mn, and Cu levels in the roots and shoots of WT, *cb1/4/5/8/9*, and *cipk3/9/23/26* mutants, regardless of whether conditions were normal or Zn-deficiency (Fig. S2 online). Notably, an analysis of Zn concentration revealed a substantial increase in Zn levels in the roots and shoots of *cb1/4/5/8/9* and *cipk3/9/23/26* mutants specifically under Zn-deficiency conditions, with no significant changes observed in standard growth conditions (Fig. 1j, k). These findings further suggested that CBL1/4/5/8/9 and CIPK3/9/23/26 are involved in the response to Zn deficiency.

To investigate the impact of Zn deficiency on the expression patterns of CBL1/4/5/8/9 and CIPK3/9/23/26, we conducted qRT-PCR analysis and discovered that the transcriptional levels of these genes remained largely unchanged under Zn-deficiency conditions

compared to normal growth conditions (Fig. S3a online). These findings indicate that Zn deficiency does not significantly alter the transcript levels of *CBL1/4/5/8/9* and *CIPK3/9/23/26*, suggesting a potential effect at the translational level instead.

3.2. *CIPK3/9/23/26* interact with Zn transporter *ZIP12*

Given the localization of *CBL1/4/5/8/9-CIPK3/9/23/26* complexes to the plasma membrane, we chose to continue our study with the Zn transporters of the ZIP/IRT family, which are also located in the plasma membrane [14,15,33,34]. Subsequently, we employed bimolecular fluorescence complementation (BiFC) to investigate the interactions between CIPK26, which exhibited a higher transcription level in response to Zn deficiency compared to CIPK3, 9, and 23, and 11 members of the ZIP/IRT family (ZIP2–6, 9–10, 12, and IRT1–3). Our findings revealed fluorescence signals upon co-expression of CIPK26 with ZIP2, ZIP3, ZIP4, ZIP9, ZIP10, ZIP12, and IRT1 (Fig. 2a, b). Notably, the signals with ZIP2, ZIP4, and ZIP9 were robust, with ZIP12 exhibiting the strongest signal among them. Given ZIP2's unique role in Zn transport within root columnar sheath cells, distinct from ZIP4, ZIP9, and ZIP12's function in Zn uptake [9,21], we further characterized Zn deficiency phenotypes in *zip4*, *zip9*, and *zip12* single mutants, as well as *zip4/9*, *zip4/12*, *zip9/12* double mutants, and *zip4/9/12* triple mutants. The results indicated that all single mutants displayed Zn deficiency sensitivity, with *zip12* being the most sensitive. Moreover, double mutants exhibited heightened sensitivity compared to single mutants, and the *zip4/9/12* triple mutant displayed the most pronounced Zn deficiency sensitivity (Fig. 2c–h). Notably, ZIP12 transcription was upregulated by several hundredfold in response to Zn deficiency, significantly exceeding the upregulation observed for ZIP4 and ZIP9 [9,16]. We conducted a comprehensive investigation into the transcription levels of ZIP2, ZIP4, ZIP9, and ZIP12 in response to Zn-deficiency stress. After growing wild-type material on Hoagland medium for seven days, we subjected it to Zn-deficiency conditions for durations of 0 h, 6 h, 12 h, 1 d, 3 d, and 5 d. Our findings aligned with existing literature, demonstrating that ZIP12 exhibited the most significant upregulation in transcription level in response to Zn-deficiency stress (Fig. S3b online). Consequently, based on these observations, we selected ZIP12 (*zip12-1* SALK_137184) as the primary downstream target for our CBL-CIPK research.

Taking into account the functional redundancy of CIPK3/9/23/26 in the Zn-deficiency signal transduction pathway, we proceeded to analyze whether CIPK3/9/23/26 interacts with ZIP12. Using the plasma membrane marker *CBL1-OPF* for BiFC detection [35], we found that co-expression of CIPK3/9/23/26 and ZIP12 proteins (and the positive control CIPK23+NRAMP1) in tobacco leaves produced strong fluorescence signals, which was co-localized with the fluorescence signals of the plasma membrane localization reporter gene *CBL1-OPF*, while the negative controls (CIPK3/9/23/26+GUS/GUS+ZIP12) and (CIPK8+ZIP12) resulted in no fluorescence signals (Fig. 3a, b and Fig. S4a, b online). These results showed that CIPK3/9/23/26 interacted with ZIP12 on the plasma membrane.

We then utilized the split-luciferase complementation (LCI) assay to verify the authenticity of the interactions described above. Fluorescence signal was detected only in the tobacco leaf region where CIPK3/9/23/26 and ZIP12 (and the positive control CIPK23+NRAMP1) proteins were co-expressed (Fig. 3c and Fig. S4c, d online). Furthermore, we conducted a Co-immunoprecipitation (Co-IP) assay in *Arabidopsis* root to investigate whether CIPK26 interacts with ZIP12. Total proteins were extracted from CIPK26-FLAG/ZIP12-GFP, GUS-FLAG/ZIP12-GFP, CIPK26-FLAG/GFP transgenic plants and immunoprecipitated using agarose-conjugated anti-GFP antibody. Consistently, ZIP12-GFP effectively immunoprecipi-

tated CIPK26-FLAG in CIPK26-FLAG/ZIP12-GFP transgenic plants (Fig. 3d). Collectively, these findings demonstrated that CIPK3/9/23/26 interacts with ZIP12 both *in vitro* and *in vivo*.

3.3. *CIPK3/9/23/26* primarily phosphorylate ZIP12 at Ser185

As a protein kinase, CIPK facilitates signal transduction by phosphorylating downstream substrates [30,36]. Consequently, we embarked on an investigation to determine if CIPK26 phosphorylates ZIP12, which harbors nine transmembrane regions, rendering full-length protein purification challenging. Hence, we focused on the largest Loop domain (143–200 aa) within ZIP12 and identified four potential phosphorylation sites—Ser148, Thr156, Ser178, and Ser185—based on predictions from the phosphorylation prediction tool (<https://gps.biocuckoo.cn/online.php>) (Fig. 4a). Our *in vitro* phosphorylation assay revealed that CIPK26 indeed phosphorylates the ZIP12-Loop domain, with the Ser185 site exhibiting the most pronounced reduction in phosphorylation signal upon mutation to alanine (Ala). Although mutations at Ser148 and Ser178 also slightly diminished phosphorylation, the effect was less pronounced compared to Ser185 (Fig. 4b). Subsequently, our study prioritized Ser185 for further analysis. Notably, CIPK3, CIPK9, and CIPK23, three additional protein kinases, were also found to phosphorylate ZIP12-Loop, and the phosphorylation signal was significantly weakened when Ser185 was mutated in ZIP12-Loop (Fig. 4c). These findings underscore the primary role of CIPK3/9/23/26 in phosphorylating ZIP12 at the Ser185 residue.

To investigate the conservation of the Ser residues in positions corresponding to Ser185 in other ZIP/IRT family members, we first performed a phylogenetic analysis of 15 *Arabidopsis* ZIP/IRT transporters. The comparative analysis reveals that Ser185 is conserved in ZIP1/2/8/12, substituted by Thr in IRT2, and not conserved in other members of the ZIP/IRT family (Fig. S5a online). Additionally, the phylogenetic tree we constructed provides further support for this observation (Fig. S5b online). Furthermore, to assess the conservation of the Ser185 residue across various species, we retrieved 26 protein sequences homologous to *Arabidopsis* ZIP12 from NCBI. The alignment analysis revealed a significant conservation of Ser185 among various species, underscoring its evolutionary importance (Fig. S5c–e online). Our findings suggest that the phosphorylation of Ser185 in ZIP12 by CIPK3/9/23/26 is partially conserved within the *Arabidopsis* ZIP/IRT family but highly conserved across different species, highlighting its evolutionary significance.

To elucidate the potential regulatory function of phosphorylation in ZIP12 activity under Zn-deficiency, we evaluated the phosphorylation status of ZIP12 upon exposure to Zn-deficiency conditions. Specifically, we subjected 7-day-old CIPK26-overexpressing (CIPK26-OE) transgenic plants to varying durations (0 h, 6 h, 12 h, 1 d, 3 d, 5 d) of Zn deficiency. Following this, we purified FLAG-tagged CIPK26 proteins and performed protein kinase assays using GST-ZIP12-Loop fusion proteins labeled with [γ -³²P] ATP. Our results demonstrated a significant increase in the phosphorylation level of ZIP12-Loop by CIPK26 from 12 h to 3 d of Zn deficiency, followed by a gradual decline thereafter (Fig. 4d). These observations suggest that CIPK26-mediated phosphorylation of ZIP12 is induced by Zn deficiency stress, potentially modulating ZIP12's functionality under such conditions.

To further determine whether CIPK3/9/23/26-mediated ZIP12 phosphorylation occurs in plants in response to Zn deficiency, we performed time series analysis on the phosphorylation level of ZIP12 under Zn deficiency conditions. ZIP12-GFP/WT#6, ZIP12^{S185A}-GFP/WT#8 and ZIP12-GFP/*cipk3/9/23/26*#10 transgenic plants were treated with Zn deficiency for 0 h, 6 h, 12 h, 1 d, 3 d, 5 d, respectively. To specifically detect the phosphorylation bands of ZIP12, we first incubated the samples with anti-GFP agarose beads to enrich the ZIP12-GFP protein. Subsequently,

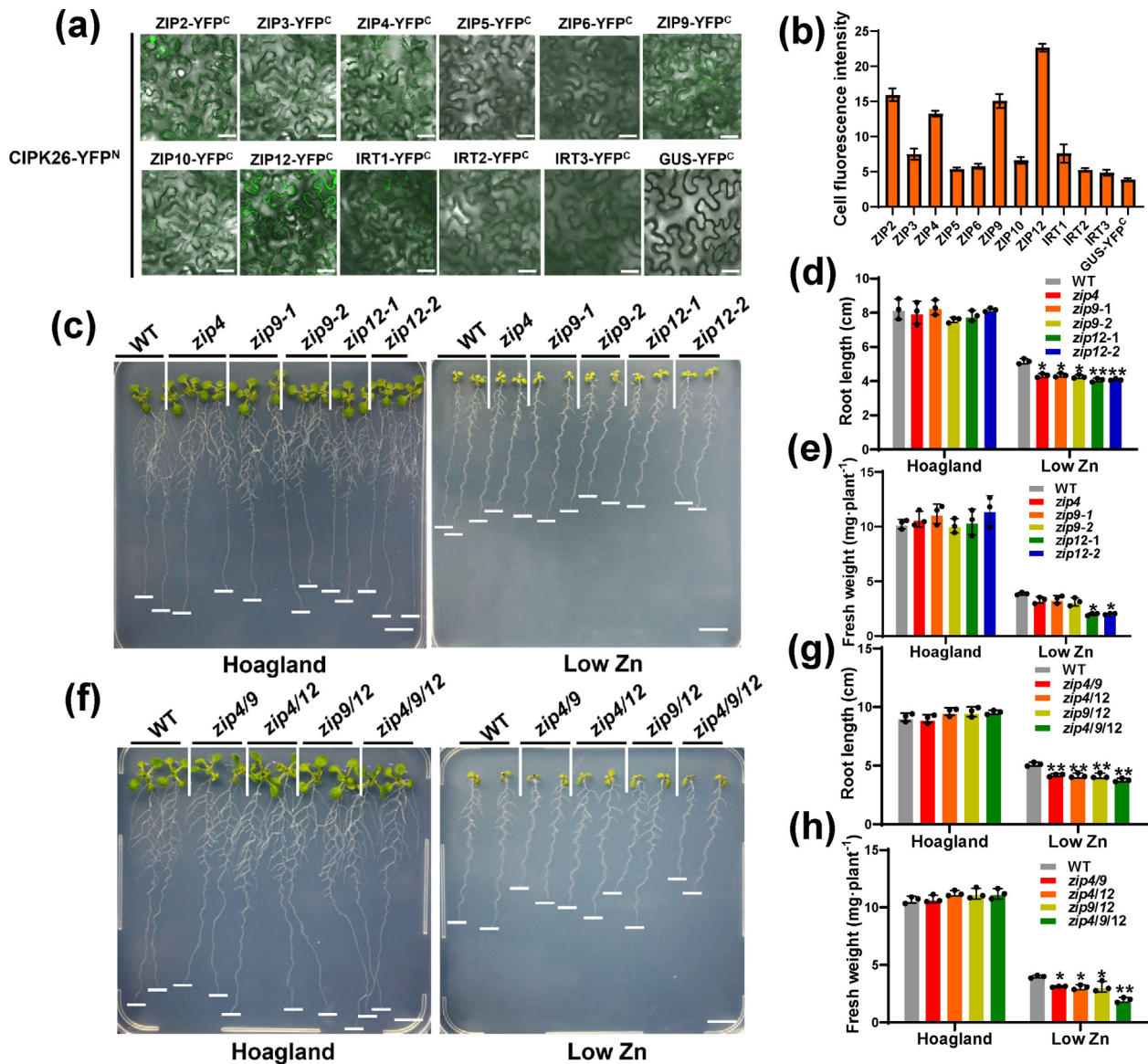


Fig. 2. Interaction screening of CIPK26 with plasma membrane-localized ZIP family member proteins and Zn deficiency phenotypes of single, double and triple mutants of *zip4*, *zip9*, *zip12*. (a) Partial yellow fluorescent protein (YFP) constructs were fused with CIPK26 or ZIPs, and the fusions were co-expressed in *N. benthamiana* leaves. The YFP signal was visualized using confocal microscopy. Scale bars, 40 μ m. (b) Imagej was used for statistical analysis of the YFP signals shown in (a). (c) Zn deficiency phenotype *zip4*, *zip9*, and *zip12* single mutants. The plants were grown under Hoagland and Zn-deficiency medium for 10 d. Scale bars, 1 cm. (d and e) Statistical analysis of the root lengths and the fresh weights of the plants shown in (c). (f) Zn deficiency phenotype *zip4/9*, *zip4/12*, *zip9/12* and *zip4/9/12* mutants. The plants were grown under Hoagland and Zn-deficiency medium for 10 d. Scale bars, 1 cm. (g and h) Statistical analysis of the root lengths and the fresh weights of the plants shown in (f). Bars present the mean \pm SD ($n = 3$ independent biological replicates, 16 seedlings; * $P < 0.05$, ** $P < 0.01$; Student's *t* test).

we used anti-P-Ser to detect the phosphorylation signal of ZIP12 and employed anti-GFP antibody immunoblotting to quantify the protein. The results showed that the phosphorylation level of ZIP12 in *ZIP12*^{S185A}-GFP/WT#8 and *ZIP12*-GFP/*cipk3/9/23/26*#10 transgenic plants was significantly lower than that in *ZIP12*-GFP/WT#6 plants. In addition, we observed that the phosphorylation of ZIP12 was significantly enhanced in *ZIP12*-GFP/WT#6 transgenic plants after 12 h of Zn deficiency treatment (Fig. 4e and Fig. S6a online). The temporal pattern and magnitude of ZIP12 phosphorylation closely mirrored the activation of CIPK26, which likewise commenced at 12 h of Zn deficiency and persisted until 3 d. These findings imply that Ser185 phosphorylation of ZIP12 in response to Zn deficiency is contingent upon the activation of CIPK3/9/23/26 kinases, with their activity escalating from the 12-hour mark of Zn deprivation.

3.4. CIPK3/9/23/26-mediated Ser185 phosphorylation is crucial for maintaining the protein stability of ZIP12 under Zn deficiency

Next, we delved into the mechanism behind ZIP12^{Ser185} phosphorylation's impact on the plant's response to Zn deficiency stress. Initially, we investigated whether this residue affected the stability of ZIP12 under Zn-deficiency conditions. To this end, we grew *ZIP12*-GFP/WT#6 and *ZIP12*^{S185A}-GFP/WT#8 transgenic plants on Hoagland medium for 7 d and then transferred them to Zn-deficiency medium for various time periods (0 h, 6 h, 12 h, 1 d, 3 d, 5 d). We then assessed the protein accumulation of ZIP12. Western blot analysis revealed that under Zn deficiency conditions, ZIP12 protein accumulation decreased from 12 h onwards as the duration of Zn deficiency treatment increased. In contrast, the protein accumulation of ZIP12^{S185A} remained relatively constant

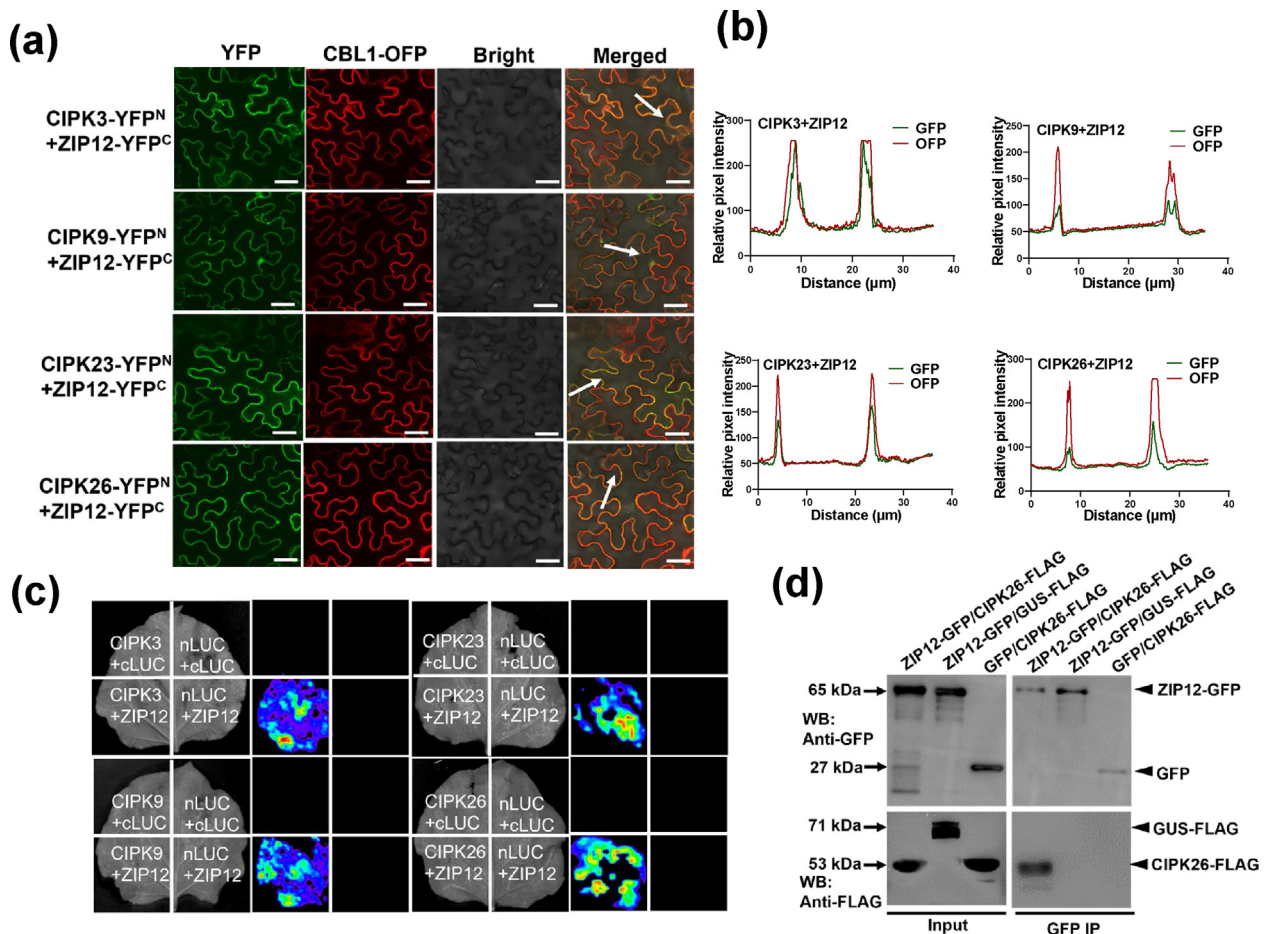


Fig. 3. CIPK3/9/23/26 interact with ZIP12. (a) BiFC assay showing the interaction between CIPK3/9/23/26 and ZIP12. Vectors encoding CIPK3/9/23/26-YFP^N and ZIP12-YFP^C were constructed and co-expressed with CBL1-OFP (a plasma membrane marker) in *N. benthamiana*. Scale bars, 40 μm. The fluorescence intensity (OFP and GFP signals) was scanned using CellSense software. (b) Fluorescence intensity analysis of the location of the interaction between CIPK3/9/23/26-YFP^N and ZIP12-YFP^C in *N. benthamiana* cells. The fluorescence intensity (mCherry/OFP and GFP signals) of the section lines was scanned using Fiji/IMAGEJ software. The location of the section line is marked in (a). (c) LCI assay showing the interaction between CIPK3/9/23/26 and ZIP12. ZIP12-cLUC/GUS-nLUC, GUS-cLUC/CIPK3/9/23/26-nLUC, and GUS-cLUC/GUS-nLUC were used as negative controls. (d) Co-immunoprecipitation of CIPK26 with ZIP12 in ZIP12-GFP/CIPK26-FLAG transgenic plants. The ZIP12-GFP/GUS-FLAG and GFP/CIPK26-FLAG transgenic plants served as negative controls. The experiments were repeated independently at least three times, with consistent results. The experiments were repeated three times (a–d) with similar results.

throughout the duration of Zn deficiency treatment (Fig. 4f and Fig. S6b online). Furthermore, treating the plants with the 26S proteasome inhibitor MG132 significantly blocked the decrease in ZIP12-GFP protein level caused by Zn deficiency. When cycloheximide (CHX) was used to block protein synthesis, protein levels still began to decrease at 12 h (Fig. 4g). Collectively, these findings indicated that CIPK3/9/23/26 phosphorylation of Ser185 in ZIP12 affects the stability of ZIP12 protein under Zn deficiency conditions, which is dependent on the ubiquitin/26S proteasome-mediated protein degradation pathway.

To further investigate whether the subcellular localization of ZIP12 is influenced by Zn supply, we subcloned the constructs containing ZIP12-GFP, ZIP12^{S185A}-GFP and ZIP12^{S185D}-GFP under the control of 35S promoter into *zip12* mutants. The transgenic lines were selected (ZIP12-GFP#1, ZIP12^{S185A}-GFP#2, ZIP12^{S185D}-GFP#2) and have been tested by qRT-PCR and the expression levels are all around 4 times higher (Fig. S7a online), exhibiting moderate and consistent expression, thereby minimizing potential interference from other variables. Confocal microscopy analysis showed that ZIP12-GFP, ZIP12^{S185A}-GFP and ZIP12^{S185D}-GFP were primarily localized to the plasma membrane of *Arabidopsis*, and the localization of ZIP12 was not altered by Zn deficiency (Fig. S7b–d online).

We also employed *zrt1zrt2* mutant to investigate whether phosphorylation at Ser185 impacts the yeast transport activity of ZIP12 [37]. We performed the experiment following the methodologies outlined in previously published research [15]. The results revealed that both ZIP12 and its variants could compensate for the growth defects of *Δzrt1zrt2* on SD-Ura medium and SD-Ura +5 mmol/L EGTA medium (Zn deficiency), and there was no significant difference in the yeast growth phenotype between the normal form of ZIP12 and its variants under normal and Zn deficiency conditions (Fig. S8 online). Collectively, these results indicate that the Ser185 residue does not affect the subcellular localization and yeast transport activity of ZIP12.

To verify whether Ser185 phosphorylation plays a physiological role in plants, we generated transgenic lines *zip12*/ZIP12, *zip12*/ZIP12^{S185A}, and *zip12*/ZIP12^{S185D}. Phenotypic analysis revealed that the *zip12*/ZIP12^{S185A} lines exhibited greater tolerance compared to WT and *zip12*/ZIP12 plants under Zn-deficiency conditions. Conversely, the *zip12*/ZIP12^{S185D} line was more sensitive than WT and *zip12*/ZIP12 plants, resembling the sensitivity of the *zip12* single mutant (Fig. 5a–d). To further confirm that the observed phenotypes were caused by Zn deficiency, the concentrations of Zn, Fe, Mn, and Cu in *zip12*, *zip12*/ZIP12, *zip12*/ZIP12^{S185A}, *zip12*/ZIP12^{S185D}

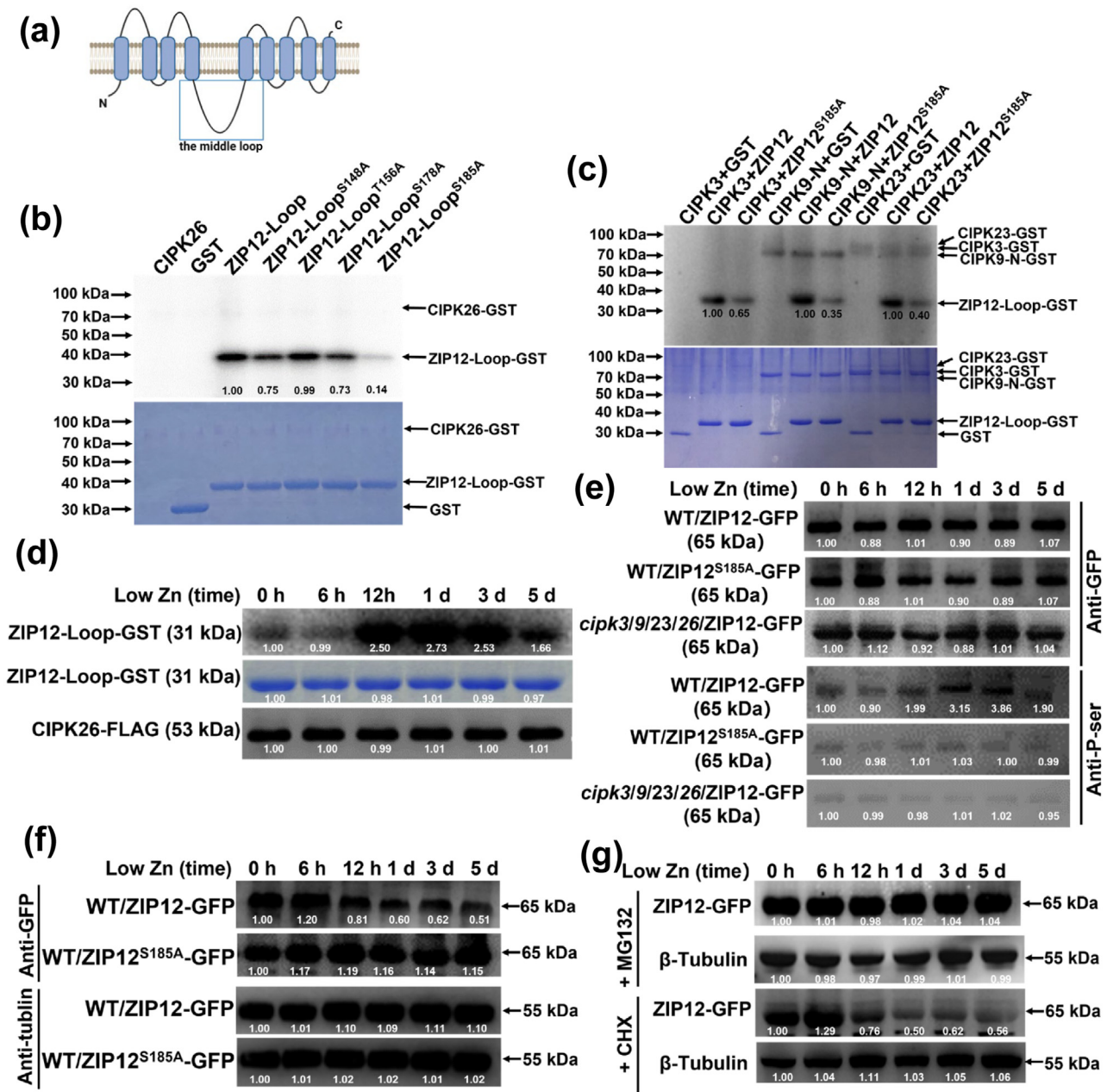


Fig. 4. CIPK3/9/23/26 phosphorylate ZIP2 at Ser185 and affects its protein stability. (a) The diagram illustrates the transmembrane structure of ZIP2. (b) CIPK26 phosphorylates ZIP12 *in vitro*. Ser185 is essential for the phosphorylation of ZIP12 by CIPK26. Recombinant purified GST-CIPK26 was incubated with GST-ZIP12-Loop, its mutant forms, or GST in kinase reaction buffer with 1 μ Ci [γ -³²P] ATP for 30 min at 30 °C. The proteins were separated by SDS-PAGE. Top, autoradiograph; bottom, CBB staining. (c) CIPK3/9/23 phosphorylates ZIP12 *in vitro*. Ser185 is essential for the phosphorylation of ZIP12 by CIPK3/9/23. Recombinant purified GST-CIPK3/9-N/23 was incubated with GST-ZIP12-Loop, GST-ZIP12^{S185A}-Loop, or GST in kinase reaction buffer with 1 μ Ci [γ -³²P] ATP for 30 min at 30 °C. The proteins were separated by SDS-PAGE. Top, autoradiograph; bottom, CBB staining. (d) Seven-day-old *Arabidopsis* seedlings were treated with a Zn-deficiency medium for the indicated time periods. The protein kinases were quantified by SDS-PAGE and are shown at the bottom. Top, autoradiograph; middle, CBB staining; bottom, western blot imaging. (e) Seven-day-old seedlings were treated under Zn-deficiency conditions for 0 h, 6 h, 12 h, 1 d, 3 d and 5 d, respectively. The phosphorylation signals of ZIP12 were detected by anti-P-Ser antibodies and anti-GFP antibody. (f) ZIP12 and ZIP12^{S185A} protein levels under different durations of Zn deficiency. WT/ZIP12-GFP and WT/ZIP12^{S185A}-GFP transgenic plants grown under Hoagland conditions for 7 d were transferred to Zn-deficiency condition for 0 h, 6 h, 12 h, 1 d, 3 d, 5 d respectively. ZIP12-GFP and ZIP12^{S185A}-GFP proteins were detected by immunoblotting using an anti-GFP antibody. Tubulin protein is used as internal reference protein. (g) Effect of MG132 and CHX treatment on ZIP12. WT/ZIP12-GFP transgenic plants grown under Hoagland conditions for 7 d were transferred to Zn-deficiency conditions were treated with MG132 and CHX for 0 h, 6 h, 12 h, 1 d, 3 d and 5 d. Tubulin protein is used as internal reference protein. The experiments were repeated independently at least three times, with consistent results.

and WT plants were determined. Notably, *zip12/ZIP12^{S185A}* plants cultivated in Zn-deficiency solution exhibited greater tolerance, while *zip12/ZIP12^{S185D}* plants were more sensitive compared to WT (Fig. 5e–g). Under Zn-deficiency conditions, the Zn concentration in the roots and shoots of *zip12/ZIP12^{S185A}* plants was significantly higher than in WT. Conversely, the Zn concentration in the

shoots of *zip12/ZIP12^{S185D}* plants was significantly lower than in WT (Fig. 5h, i). The concentrations of Fe, Mn, and Cu in these plants showed no significant differences under both Zn deficiency and normal conditions (Fig. S9a–f online). Collectively, these findings highlight the critical role of Ser185 phosphorylation in plant growth and physiology.

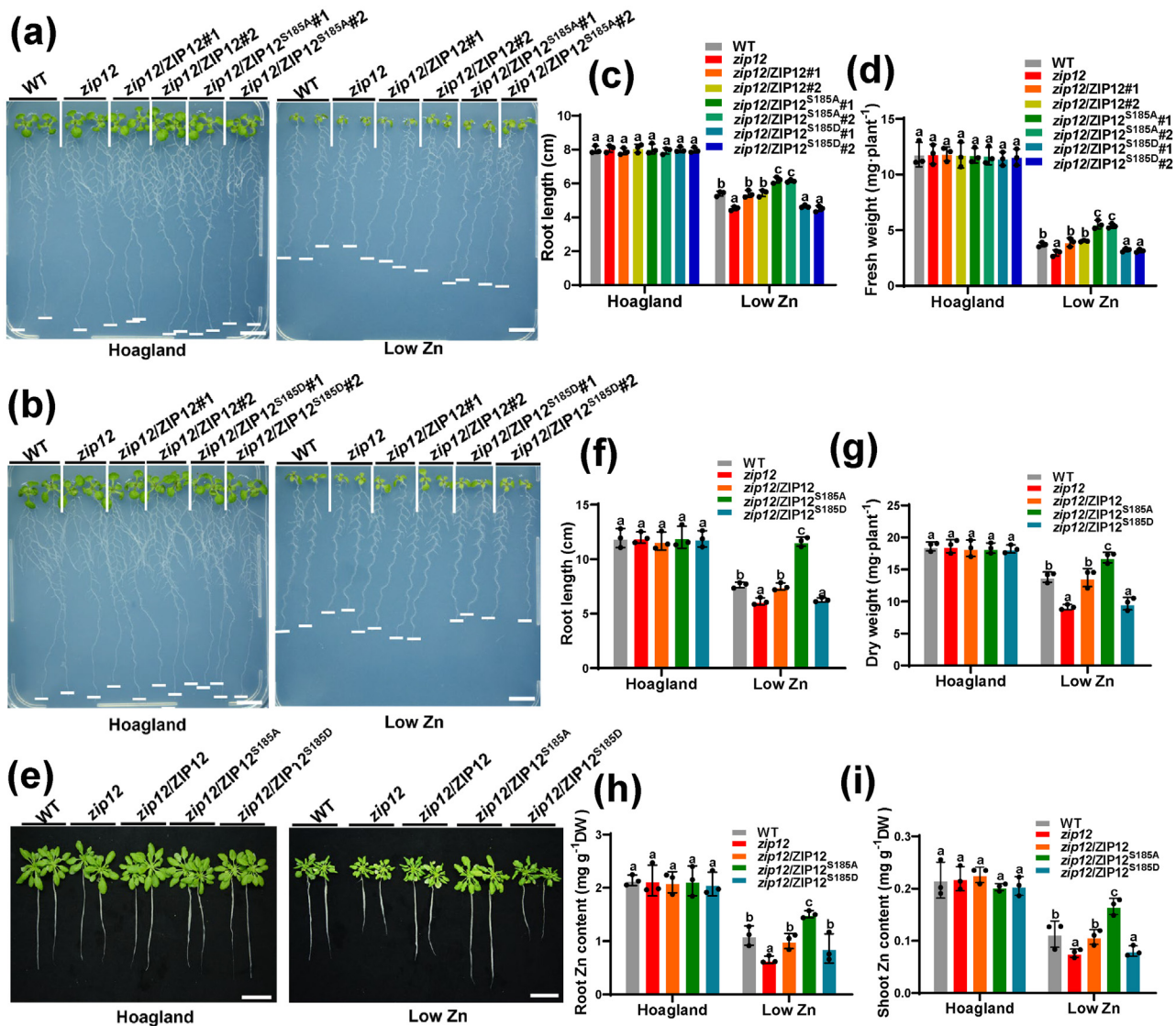


Fig. 5. Functional analysis of ZIP12 phosphorylated by CIPK3/9/23/26. (a and b) Zn-deficiency phenotypes of *zip12*, *zip12/ZIP12*, *zip12/ZIP12^{S185A}*, and *zip12/ZIP12^{S185D}* transgenic plants. Plants grew on Hoagland and Zn-deficiency medium for 10 d. Scale bars, 1 cm. (c and d) Statistical analysis of root lengths and fresh weights of plants shown in (a and b). (e) Phenotypic analysis *zip12*, *zip12/ZIP12*, *zip12/ZIP12^{S185A}*, and *zip12/ZIP12^{S185D}* transgenic plants in hydroponic culture and treated for 2 weeks with low Zn culture solution. Scale bars, 3 cm. (f and g) Statistical analysis of root lengths and dry weights of plants shown in (e). (h and i) Statistical analysis of Zn concentrations of plants in Hoagland and Zn-deficiency hydroponic culture shown in (e). Bars represent the mean \pm SD ($n = 3$ independent biological replicates). a and b, 16 seedlings. e, 6 seedlings). Statistical differences were calculated by one-way ANOVA. Different letters indicate means that were statistically different by Tukey's multiple testing method ($P < 0.05$).

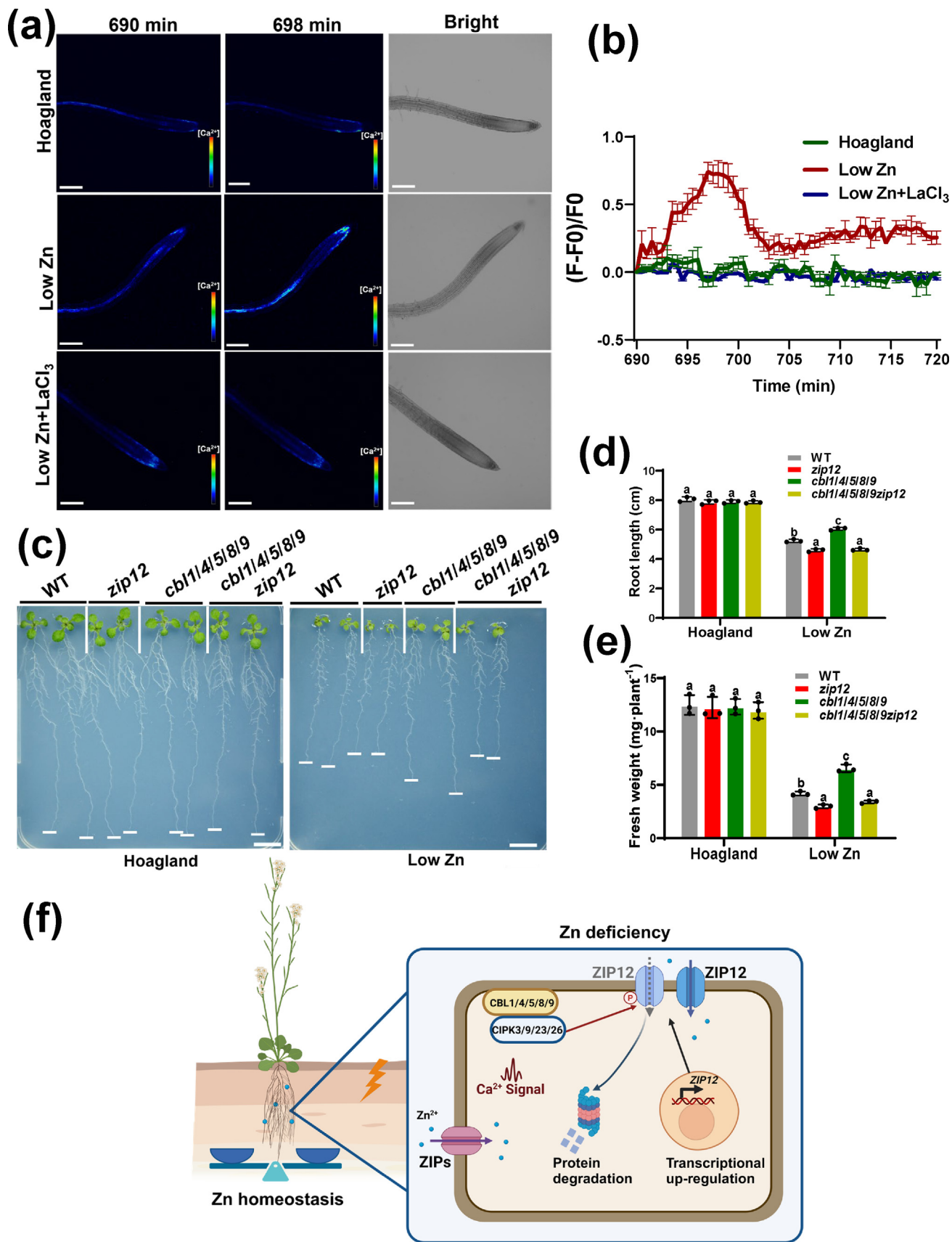
3.5. CBL1/4/5/8/9-CIPK3/9/23/26 complex negatively regulates the response of ZIP12 to Zn deficiency

If CBL1/4/5/8/9-CIPK3/9/23/26 negatively regulates the response of ZIP12 to Zn deficiency, once the Zn deficiency stress subsides, it may accelerate the recovery of plants. We observed the Zn deficiency compensation growth phenotype and high Zn growth phenotype of *cbl1/4/5/9*, *cbl1/4/5/8/9*, *cipk3/9/23/26*, and *zip12* mutants. The Zn deficiency complementation experiment results revealed that the tolerance growth phenotype of *cbl1/4/5/9*, *cbl1/4/5/8/9*, *cipk3/9/23/26* and the sensitive growth phenotype of *zip12* on Zn deficiency medium were restored to a similar level as WT (Fig. S10a–c online). However, when grown on high-Zn media, the mutants *zip4*, *zip9*, *zip12*, *zip4/9*, *zip4/12*, *zip9/12*, *zip4/9/12*, as well as *cbl1/4/5/8/9*, *cipk3/9/23/26*, and *cbl1/4/5/8/9/zip12* did not exhibit significant differences in root length or fresh weight compared to the wild type (Fig. S10d–i

and Fig. S11a–f online). Furthermore, we analyzed the Zn content of selected mutants, including *cbl1/4/5/9*, *cbl1/4/5/8/9*, *cipk3/9/23/26*, *zip12*, and *cbl1/4/5/8/9/zip12*, under high Zn (500 $\mu\text{mol/L}$) culture conditions. Our results showed no significant variations in Zn content compared to the wild type (Fig. S11g, h online). These findings further corroborate that the Ca^{2+} -CBL1/4/5/8/9-CIPK3/9/23/26 signaling pathway primarily functions to negatively regulate ZIP12 in response to Zn deficiency stress.

3.6. Zn deficiency stimulates an obvious Ca^{2+} signal in Arabidopsis roots

A significant body of research has established the critical role of Ca^{2+} signaling in regulating plant nutrient uptake, transport, and response to various nutrient stresses [38]. However, whether Zn deficiency can trigger Ca^{2+} signal transduction in plants remains



unexplored. To this end, we utilized wild-type *Arabidopsis* plants stably transformed with the *GCaMP6s* gene. *GCaMP6s* is a highly sensitive fluorescent protein that accurately reflects changes in intracellular free Ca^{2+} concentration [39,40]. Given that long-term laser irradiation can lead to fluorescence quenching, it was not technically feasible for us to record continuously for 12 h. Based on published research methods for Mn deficiency stress-induced Ca^{2+} signaling, continuous recording for 6 h represents the limit [41].

Furthermore, our data indicate that CIPK3/9/23/26 proteins enhance the phosphorylation of ZIP12 at approximately 12 h of Zn deficiency, suggesting that CBL1/4/5/8/9-CIPK3/9/23/26 proteins sense Ca^{2+} signals at this time point and phosphorylate ZIP12. We collected data every 30 s and observed it under a laser confocal microscope at 11.5–12 h. The results revealed a significant enhancement of fluorescence signal in the cytoplasm of the root elongation zone of *Arabidopsis* at 698 min under Zn deficiency conditions. In contrast, the fluorescence signal of *Arabidopsis* roots treated on normal Hoagland medium and treated with 50 $\mu\text{mol/L}$ Ca^{2+} channel blocker LaCl_3 did not change significantly during the period of 11.5–12 h (Fig. 6a, b and Movies S1–S3 online). These findings demonstrated that Zn deficiency can indeed induce a Ca^{2+} signal in *Arabidopsis*, supporting our hypothesis that CBL1/4/5/8/9-CIPK3/9/23/26 proteins can perceive and transmit this Ca^{2+} signal at approximately 12 h of Zn deficiency.

3.7. CBL1/4/5/8/9 act upstream of ZIP12

We observed tolerance to Zn deficiency in *cb1/4/5/8/9* and *cipk3/9/23/26* mutants, whereas the *zip12* single mutant exhibited a sensitive phenotype. Additional experiments demonstrated an interaction between CBL1/4/5/8/9-CIPK3/9/23/26 and ZIP12. To elucidate the genetic relationship between CBL1/4/5/8/9 and ZIP12, we generated higher-order mutants by crossing *cb1/4/5/8/9* with the *zip12* mutant and examined their Zn deficiency phenotypes. The resulting *cb1/4/5/8/9/zip12* mutants exhibited a Zn deficiency sensitive phenotype similar to the *zip12* mutant (Fig. 6c–e). These findings indicate that CBL1/4/5/8/9 function upstream of ZIP12.

4. Discussion and conclusion

Zn is an essential trace element for plant growth and development. Previous studies have only reported that changes in exogenous Zn concentration can cause fluctuations in the protein expression of some members of the Ca^{2+} sensor family [42]. However, it is not clear whether Zn deficiency stress can cause a recognizable Ca^{2+} signal that triggers CBLs and their target protein

kinase CIPKs in *Arabidopsis* to form a phosphorylation cascade. Our study sheds light on this by demonstrating that the CBL1/4/5/8/9-CIPK3/9/23/26 complex has the ability to detect such Ca^{2+} signals, specifically phosphorylating the Ser185 residue of ZIP12 at 12 h of Zn deficiency, which subsequently triggers ZIP12 protein degradation. Overall, this Ca^{2+} -CBL1/4/5/8/9-CIPK3/9/23/26-ZIP12 signaling pathway plays a key role in maintaining Zn homeostasis in plants.

4.1. CBL1/4/5/8/9-CIPK3/9/23/26 has functional redundancy in response to Zn deficiency

CBLs are Ca^{2+} sensors that interact with their target kinase protein CIPK, phosphorylate various downstream substrates, and regulate their activity [20,43]. Among them, CBL4-CIPK24 synergistically regulates the activity of plasma membrane Na^+/H^+ transporter SOS1 [44]. The CBL1/9-CIPK23 complex orchestrates the uptake of K^+ , NO_3^- , and NH_4^+ by phosphorylating AKT1, CHL1/NRT1.1, and AMT1 [45–47]. Furthermore, it regulates the transport of micronutrient metal cations. Noteworthy is the inactivation of the primary high-affinity iron uptake transporter (IRT1) within the *Arabidopsis* ZIP/ITR family by CBL1/9-CIPK23, safeguarding plants from damage caused by highly reactive metals [48]. Moreover, the removal of the high-affinity Mn^{2+} uptake system NRAMP1 from the plasma membrane in the presence of Mn^{2+} necessitates CBL1/9-CIPK23 [24]. The CBL2/3-CIPK3/9/23/26 complex regulates intracellular Mg^{2+} , K^+ and Mn^{2+} homeostasis [20,25,33,49]. Finally, CBL1/9-CIPK11 activates the activity of bHLH transcription factor FIT by activating iron absorption in *Arabidopsis*, and then regulate plant iron nutrition [50].

A pivotal finding of our study is that plasma membrane-localized *cb1/4/5/8/9* and *cipk3/9/23/26* mutants were able to respond to Zn deficiency (Fig. 1). This observation aligns with previous reports outlining the formation of a CBL-CIPK regulatory network, where CBL1,4,5,8,9 can interact with CIPK3/9/23/26 members [32], enabling CBL1/4/5/8/9 to activate and recruit CIPK3/9/23/26 to the plasma membrane in response to Zn deficiency. Notably, the absence of overt Zn deficiency phenotypes in *cb1*, *cipk* single, and double mutants underscores the functional redundancy of CBL1/4/5/8/9 and CIPK3/9/23/26 in regulating plant Zn homeostasis (Fig. S1 online), highlighting their collective importance in mitigating Zn deficiency stress.

4.2. CIPK3/9/23/26 interacts with and phosphorylates plasma membrane Zn transporter ZIP12

The localization of CBL1/4/5/8/9-CIPK3/9/23/26 in the plasma membrane and the Zn deficiency tolerance phenotype of

Fig. 6. Zn deficiency stimulates an obvious Ca^{2+} signal in *Arabidopsis* roots and genetic interaction of CBL1/4/5/8/9 with ZIP12. (a) Zn deficiency induces an obvious Ca^{2+} signal in *Arabidopsis* roots. The transgenic *GCaMP6s* seedlings were grown on Hoagland medium for 4 d, and then transferred to Hoagland and low Zn medium (or in low Zn medium containing 50 $\mu\text{mol/L}$ LaCl_3) for 11.5 h. The fluorescence changes of Ca^{2+} signal in *Arabidopsis* roots were continuously observed by laser confocal microscopy for half an hour. 690 min is the beginning of recording fluorescence, and 698 min is the strongest fluorescence under Zn deficiency conditions. Hoagland as a negative control. The stronger the fluorescence intensity, the higher the concentration of Ca^{2+} . Scale bar, 120 μm ($n = 3$ biological replicates). (b) Traces of average Ca^{2+} signals stimulated by different treatments in the roots of *GCaMP6s* transgenic plants are shown in (a). The fluorescence signal was collected every 30 s. F_0 was the root fluorescence value at 360 min, and $(F-F_0)/F_0$ was relative fluorescence intensity. (c) Zn deficiency phenotype of WT plants and *zip12*, *cb1/4/5/8/9*, *cb1/4/5/8/9/zip12*. Plants grew on Hoagland and low Zn medium for 10 d. Scale bars, 1 cm. (d and e) Statistical analysis of the root lengths and the fresh weights of the plants shown in (c). (f) The working model of Ca^{2+} -CBL1/4/5/8/9-CIPK3/9/23/26-ZIP12 signal pathway. When plants are in a Zn-deficiency environment, their stress response leads to a significant upregulation of the transcription levels of transporters responsible for Zn uptake (such as ZIP4, ZIP9, ZIP12), facilitating the absorption of Zn from the soil. As the fold increase in transcription levels is several hundred or even a thousand times, plants may be trying to avoid excessive expression of ZIP transporters leading to disruptions, or they may not require such high expression levels and need to appropriately reduce protein levels. The CBL-CIPK complex senses specific calcium signals, phosphorylates ZIP12, and triggers partial degradation of the ZIP12 protein. This negative feedback mechanism fine-tunes the plant's response to Zn-deficiency environments, enabling efficient resource utilization and maintaining Zn homeostasis under Zn deficiency conditions. Bars present the mean \pm SD ($n = 3$ independent biological replicates, 16 seedlings). Statistical differences were calculated by one-way ANOVA. Different letters indicate means that were statistically different by Tukey's multiple testing method ($P < 0.05$). (Created with BioRender.com).

cbl1/4/5/8/9 and *cipk3/9/23/26* high-order mutants led us to investigate whether plasma membrane-localized Zn transporters of the ZIP/IRT family could be potential targets for regulation by these CBL-CIPK complexes. Given the robust interaction observed between ZIP12 and CIPK26, coupled with the heightened sensitivity displayed by the *zip12* single mutant compared to *zip4* and *zip9*, and the remarkable upregulation of ZIP12 transcription by several hundredfold under Zn deficiency, we have determined that ZIP12, localized in the plasma membrane, serves as an optimal research target for investigating Zn homeostasis mechanisms in plants.

While previous research has reported Zn deficiency as a stimulus for root elongation in plants, enhancing Zn exploration in deeper soil layers [51]. Our findings and those of several other studies diverge significantly from this notion. Instead, numerous investigations have consistently shown that Zn deficiency leads to reduced plant biomass, including shortened root length [8,9,15]. We posit that the discrepancy arises from the varying Zn-deficiency media employed across studies. Notably, while previous studies on the *zip12* single mutant reported a subtle Zn deficiency phenotype with statistically significant root length reduction [9], our study observed a more pronounced sensitivity to Zn deficiency in the *zip12* mutant. This discrepancy may also stem from the different Zn-deficiency media used. To further validate our observations, we eliminated the potential confounding effect of Zn²⁺ in agar by employing a hydroponic system with Double Distilled Water (ddH₂O) and no added Zn²⁺ in the Zn-deficiency culture solution. Our results unequivocally demonstrate the heightened sensitivity of the *zip12* mutant and significantly lower Zn²⁺ concentrations in both roots and shoots compared to wild-type plants (Fig. 5). These findings underscore the potential redundancy within the ZIP family in regulating Zn homeostasis, yet emphasize the indispensable role of individual ZIP members, such as ZIP12, in maintaining optimal Zn levels in plants.

Our comprehensive analysis confirmed that the Zn transporter ZIP12 is one of the targets regulated by the CBL1/4/5/8/9-CIPK3/9/23/26 complex (Fig. 2 and Fig. 3). We identified that CIPK3/9/23/26 primarily target the Ser185 site in ZIP12 for phosphorylation, and notably, this site is highly conserved across both monocotyledonous and dicotyledonous plant species (Fig. S5 online). This observation implies that CIPK-mediated phosphorylation of ZIP12 is a widely conserved aspect of plant Zn homeostasis. Through the analysis of Zn deficiency phenotype and Zn concentration in transgenic lines with important functional sites of ZIP12 in *Arabidopsis*, it was found that they responded to Zn deficiency stress (Fig. 5). Furthermore, our investigation of the Zn deficiency compensation phenotype in *cbl1/4/5/8/9*, *cipk3/9/23/26*, and *zip12* mutants, as well as the high Zn phenotype in *zips*, *cbl1/4/5/8/9*, *cipk3/9/23/26*, and *cbl1/4/5/8/9zip12* mutants, revealed no significant differences in either phenotype or Zn content compared to the wild type (WT) (Figs. S10 and S11 online). These results imply that the Ca²⁺-CBL1/4/5/8/9-CIPK3/9/23/26 signaling pathway may play a pivotal role in regulating Zn homeostasis specifically under Zn-deficiency conditions in plants. Moreover, we did not find that the phosphorylation status of ZIP12 affects its localization and transport activity under Zn deficiency conditions (Figs. S7 and S8 online). These results also reinforce the conclusion that phosphorylation of ZIP12 at Ser185 is a key regulatory mechanism for regulating ZIP12 protein stability and precise regulation of cellular Zn homeostasis.

4.3. Zn deficiency stimulates an obvious Ca²⁺ signal in *Arabidopsis*

As a well-known plant secondary messenger, the Ca²⁺ signal has been reported to be involved in various physiological and biochem-

ical reactions [19,52,53]. Our exploration revealed that Zn deficiency treatment at 698 min can induce *Arabidopsis* roots to produce an obvious Ca²⁺ signal (Fig. 6g, h). Since Zn is a trace element and plants require only a small amount of it, calcium signals may not be observed in a short-term Zn-deficiency treatment. Studies indicate that high Mn stress can rapidly induce calcium signals in plants within 15 min, whereas Mn-deficiency stress initiates calcium signals after 120 min, displaying an oscillatory pattern [41]. Our hypothesis proposed that Zn-deficient stress could induce a gradual and fluctuating Ca²⁺ signal in plants. Given that long-term laser irradiation can lead to fluorescence quenching, it was not technically feasible for us to record continuously for 12 h. Therefore, based on the results of CIPK3/9/23/26 phosphorylating ZIP12, we investigated whether low Zn stress triggered the production of calcium signals within half an hour before CIPK3/9/23/26 began phosphorylating ZIP12.

In conclusion, we hypothesize that there may be a mechanism by which Ca²⁺-CBL1/4/5/8/9-CIPK3/9/23/26 signaling pathway regulates the degradation of the ZIP12 protein. When plants are in a Zn-deficiency environment, their stress response leads to a significant upregulation of the transcription levels of transporters responsible for Zn uptake (such as ZIP4, ZIP9, ZIP12), facilitating the absorption of Zn from the soil. As the fold increase in transcription levels is several hundred or even a thousand times, plants may be trying to avoid excessive expression of ZIP transporters leading to disruptions, or they may not require such high expression levels and need to appropriately reduce protein levels. The CBL-CIPK complex senses specific calcium signals, phosphorylates ZIP12, and triggers partial degradation of the ZIP12 protein. This negative feedback mechanism fine-tunes the plant's response to Zn-deficiency environments, enabling efficient resource utilization and maintaining Zn homeostasis under Zn deficiency conditions (Fig. 6f). This finding holds significant guiding value for future research and enhances our understanding of the Ca²⁺ signal regulation of Zn homeostasis.

Conflict of interest

The authors declare that they have no conflict of interest.

Acknowledgments

This work was supported by the National Natural Science Foundation of China (32222008 and 32300235) and China Postdoctoral Science Foundation (2023M732883) and by the Chinese Universities Scientific Fund (2452023069). We thank Dr. Jörg Kudla (Institute of Plant Biology and Biotechnology, University of Münster, 48149 Münster, Germany) for providing *cbl6*, *cbl8*, *cbl1/4/5/9*, *cbl1/4/5/8/9* mutants; Dr. Kun-Hsiang Liu for providing GCaMP6s sensor lines; Dr. Xueling Huang, Dr. Fengping Yuan, Dr. Hua Zhao, Dr. Qiong Zhang and Technician Xiaona Zhou for instrument operation guidance (State Key Laboratory for Crop Stress Resistance and High-Efficiency Production, Northwest A&F University, Yangling, China); Dr. Xiao-han Li (College of Natural Resources and Environment, Northwest A&F University) for providing technical support with ICP-MS.

Author contributions

YanJun Fang, Chuanfeng Ju, Laiba Javed, Chenyu Cao, Yuan Deng, Yaqi Gao, Xuanyi Chen, Lv Sun, and Yusheng Zhao performed this research. YanJun Fang and Chuanfeng Ju analysed the data. Cun Wang, YanJun Fang, and Chuanfeng Ju wrote the manuscript with comments from all authors.

Appendix A. Supplementary material

Supplementary data to this article can be found online at <https://doi.org/10.1016/j.scib.2025.02.010>.

References

- [1] Broadley MR, White PJ, Hammond JP, et al. Zinc in plants. *New Phytol* 2007;173:677–702.
- [2] Stanton C, Sanders D, Krämer U, et al. Zinc in plants: integrating homeostasis and biofortification. *Mol Plant* 2022;15:65–85.
- [3] Wang XT, Liu KH, Li Y, et al. Correction: zinc metalloprotease FGM35, which targets the wheat zinc-binding protein TAZNBP, contributes to the virulence of fusarium graminearum. *Stress Biol* 2024;4:49.
- [4] Lin J, Bjørk PK, Kolte MV, et al. Zinc mediates control of nitrogen fixation via transcription factor filamentation. *Nature* 2024;631:164–9.
- [5] Cakmak I, Kutman UB. Agronomic biofortification of cereals with zinc: a review. *Eur J Soil Sci* 2018;69:172–80.
- [6] Clemens S. The cell biology of zinc. *J Exp Bot* 2022;73:1688–98.
- [7] Zeng H, Wu H, Yan F, et al. Molecular regulation of zinc deficiency responses in plants. *J Plant Physiol* 2021;261:153419.
- [8] Assunção AG, Herrero E, Lin YF, et al. *Arabidopsis thaliana* transcription factors bZIP19 and bZIP23 regulate the adaptation to zinc deficiency. *Proc Natl Acad Sci USA* 2010;107:10296–301.
- [9] Inaba S, Kurata R, Kobayashi M, et al. Identification of putative target genes of bZIP19, a transcription factor essential for *Arabidopsis* adaptation to Zn deficiency in roots. *Plant J* 2015;84:323–34.
- [10] Assunção AGL. The F-bZIP-regulated Zn deficiency response in land plants. *Planta* 2022;256:108.
- [11] Ajeesh Krishna TP, Maharajan T, Victor Roch G, et al. Structure, function, regulation and phylogenetic relationship of ZIP family transporters of plants. *Front Plant Sci* 2020;11:662.
- [12] Grotz N, Fox T, Connolly E, et al. Identification of a family of zinc transporter genes from *Arabidopsis* that respond to zinc deficiency. *Proc Natl Acad Sci USA* 1998;95:7220–4.
- [13] Lin YF, Liang HM, Yang SY, et al. *Arabidopsis* IRT3 is a zinc-regulated and plasma membrane localized zinc/iron transporter. *New Phytol* 2009;182:392–404.
- [14] Milner MJ, Seamon J, Craft E, et al. Transport properties of members of the ZIP family in plants and their role in Zn and Mn homeostasis. *J Exp Bot* 2013;64:369–81.
- [15] Lee S, Lee J, Ricachenevsky FK, et al. Redundant roles of four ZIP family members in zinc homeostasis and seed development in *Arabidopsis thaliana*. *Plant J* 2021;108:1162–73.
- [16] Jain A, Sinilal B, Bhandapani G, et al. Effects of deficiency and excess of zinc on morphophysiological traits and spatiotemporal regulation of zinc-responsive genes reveal incidence of cross talk between micro- and macronutrients. *Environ Sci Technol* 2013;47:5327–35.
- [17] Lu S, Sun Y, Ma L, et al. Advancing insights into calcium homeostasis and signaling in plant growth and resilience. *Sci Bull* 2024;70:125–7.
- [18] Luan S, Wang C. Calcium signaling mechanisms across kingdoms. *Annu Rev Cell Dev Biol* 2021;37:311–40.
- [19] Dong Q, Wallrad L, Almutairi BO, et al. Ca²⁺ signaling in plant responses to abiotic stresses. *JIPB* 2022;64:287–300.
- [20] Tang RJ, Zhao FG, Yang Y, et al. A calcium signalling network activates vacuolar K⁺ remobilization to enable plant adaptation to low-K environments. *Nat Plants* 2020;6:384–93.
- [21] Wang C, Tang RJ, Kou S, et al. Mechanisms of calcium homeostasis orchestrate plant growth and immunity. *Nature* 2024;627:382–8.
- [22] Schulze S, Dubeaux G, Ceciliato PHO, et al. A role for calcium-dependent protein kinases in differential CO₂- and ABA-controlled stomatal closing and low CO₂-induced stomatal opening in *Arabidopsis*. *New Phytol* 2021;229:2765–79.
- [23] Su H, Wang T, Ju C, et al. Abscisic acid signaling negatively regulates nitrate uptake via phosphorylation of NRT1.1 by SNRK2s in *Arabidopsis*. *JIPB* 2021;63:597–610.
- [24] Zhang Z, Fu D, Xie D, et al. CBL1/9-CIPK23-NRAMP1 axis regulates manganese toxicity. *New Phytol* 2023;239:660–70.
- [25] Ju C, Zhang Z, Deng J, et al. Ca²⁺-dependent successive phosphorylation of vacuolar transporter MTP8 by CBL2/3-CIPK3/9/26 and CPK5 is critical for manganese homeostasis in *Arabidopsis*. *Mol Plant* 2022;15:419–37.
- [26] Chen X, Wang T, Rehman AU, et al. *Arabidopsis* U-box E3 ubiquitin ligase PUB11 negatively regulates drought tolerance by degrading the receptor-like protein kinases IRR1 and KIN7. *JIPB* 2021;63:494–509.
- [27] Zhang Z, Fu D, Sun Z, et al. Tonoplast-associated calcium signaling regulates manganese homeostasis in *Arabidopsis*. *Mol Plant* 2021;14:805–19.
- [28] Kumar S, Stecher G, Li M, et al. Mega x: molecular evolutionary genetics analysis across computing platforms. *Mol Biol Evol* 2018;35:1547–9.
- [29] Kudla J, Becker D, Grill E, et al. Advances and current challenges in calcium signaling. *New Phytol* 2018;218:414–31.
- [30] Batistic O, Waadt R, Steinhorst L, et al. CBL-mediated targeting of CIPKs facilitates the decoding of calcium signals emanating from distinct cellular stores. *Plant J* 2010;61:211–22.
- [31] Batistič O, Rehers M, Akerman A, et al. S-acylation-dependent association of the calcium sensor CBL2 with the vacuolar membrane is essential for proper abscisic acid responses. *Cell Res* 2012;22:1155–68.
- [32] Zhang X, Li X, Zhao R, et al. Evolutionary strategies drive a balance of the interacting gene products for the CBL and CIPK gene families. *New Phytol* 2020;226:1506–16.
- [33] Tang RJ, Zhao FG, Garcia VJ, et al. Tonoplast CBL-CIPK calcium signaling network regulates magnesium homeostasis in *Arabidopsis*. *Proc Natl Acad Sci USA* 2015;112:3134–9.
- [34] Nguyen NT, Khan MA, Castro-Guerrero NA, et al. Iron availability within the leaf vasculature determines the magnitude of iron deficiency responses in source and sink tissues in *Arabidopsis*. *Plant Cell Physiol* 2022;63:829–41.
- [35] D'Angelo C, Weini S, Batistic O, et al. Alternative complex formation of the CA-regulated protein kinase CIPK1 controls abscisic acid-dependent and independent stress responses in *Arabidopsis*. *Plant J* 2006;48:857–72.
- [36] Luan S. The CBL-CIPK network in plant calcium signaling. *Trends Plant Sci* 2009;14:37–42.
- [37] Zhao H, Eide D. The yeast ZRT1 gene encodes the zinc transporter protein of a high-affinity uptake system induced by zinc limitation. *Proc Natl Acad Sci USA* 1996;93:2454–8.
- [38] Wang T, Chen X, Ju C, et al. Calcium signaling in plant mineral nutrition: from uptake to transport. *Plant Commun* 2023;4:100678.
- [39] Chen TW, Wardill TJ, Sun Y, et al. Ultrasensitive fluorescent proteins for imaging neuronal activity. *Nature* 2013;499:295–300.
- [40] Liu KH, Niu Y, Konishi M, et al. Discovery of nitrate-CPK-NLP signalling in central nutrient-growth networks. *Nature* 2017;545:311–6.
- [41] Fu D, Zhang Z, Wallrad L, et al. Ca²⁺-dependent phosphorylation of NRAMP1 by CPK21 and CPK23 facilitates manganese uptake and homeostasis in *Arabidopsis*. *Proc Natl Acad Sci USA* 2022;119:e2204574119.
- [42] Arsova B, Amini S, Scheepers M, et al. Resolution of the proteome, transcript and ionome dynamics upon Zn re-supply in Zn-deficient *Arabidopsis*. *bioRxiv* 2019.
- [43] Batistic O, Kudla J. Plant calcineurin B-like proteins and their interacting protein kinases. *Biochim Biophys Acta* 2009;1793:985–92.
- [44] Zhu JK, Liu J, Xiong L. Genetic analysis of salt tolerance in *Arabidopsis*. Evidence for a critical role of potassium nutrition. *Plant Cell* 1998;10:1181–91.
- [45] Xu J, Li HD, Chen LQ, et al. A protein kinase, interacting with two calcineurin B-like proteins, regulates K⁺ transporter AKT1 in *Arabidopsis*. *Cell* 2006;125:1347–60.
- [46] Ho CH, Lin SH, Hu HC, et al. Chl1 functions as a nitrate sensor in plants. *Cell* 2009;138:1184–94.
- [47] Straub T, Ludewig U, Neuhäuser B. The kinase CIPK23 inhibits ammonium transport in *Arabidopsis thaliana*. *Plant Cell* 2017;29:409–22.
- [48] Dubeaux G, Neveu J, Zelazny E, et al. Metal sensing by the IRT1 transporter-receptor orchestrates its own degradation and plant metal nutrition. *Mol Cell* 2018;69:953–964.e955.
- [49] Li KL, Tang RJ, Wang C, et al. Potassium nutrient status drives posttranslational regulation of a low-K response network in *Arabidopsis*. *Nat Commun* 2023;14:360.
- [50] Gratz R, Manishankar P, Ivanov R, et al. CIPK11-dependent phosphorylation modulates fit activity to promote *Arabidopsis* iron acquisition in response to calcium signaling. *Dev Cell* 2019;48:726–40.
- [51] Sinclair SA, Senger T, Talke IN, et al. Systemic upregulation of MTP2- and HMA2-mediated Zn partitioning to the shoot supplements local Zn deficiency responses. *Plant Cell* 2018;30:2463–79.
- [52] Wang FZ, Li JF. Weitsing: a new face of Ca²⁺-permeable channels in plant immunity. *Stress Biol* 2023;3:25.
- [53] Ju C, Javed L, Fang Y, et al. *Arabidopsis* calcium-dependent protein kinases 4/5/6/11 negatively regulate hydrotropism via phosphorylation of mizu-kussei1. *Plant Cell* 2024;37:koae279.